Synthesis and Seeding Time Effect on the Inter-Crystalline Structure of Hydroxy-Sodalite Zeolite Membranes by Single Gas (H_2 and N_2) Permeation

Bayati, Behroz; Babaluo, Ali Akbar*+; Ahmadian Namini, Pejman
Nanostructure Materials Research Center (NMRC), Sahand University of Technology,
P.O. Box 51335-1996 Tabriz, I.R. IRAN

ABSTRACT: *Microporous hydroxy-sodalite zeolite membranes with different morphologies were synthesized via secondary growth technique with vacuum seeding on tubular α-Al_2O_3 supports at two different synthesis conditions (i.e. two different routes). Microstructures of the synthesized membranes were characterized by X-ray diffraction (XRD), Scanning electron microscope (SEM) and single gas permeation using H_2 and N_2. Also, the effect of seeding time on microstructure and performance of the synthesized hydroxy-sodalite top-layers was investigated at four different levels (60, 120, 180 and 240 s). Permeation test was carried out in order to attain a more exact comparison of both applied routes and seeding times. Microstructure of the synthesized hydroxy-sodalite zeolite membrane layers and the effects of the investigated factors on the elimination of inter-crystalline pores were evaluated by the permeation of single gases (H_2 and N_2) under different pressure differences at ambient temperature. The permeation results confirmed the high quality of the hydroxy-sodalite zeolite membranes manufactured via the first route at seeding time of 60s for the hydrogen purification under extremely low temperatures (< 200 K) and/or extremely high pressures (> 100 bars).*

KEY WORDS: *Hydrothermal synthesis, Inter-crystalline structure, Hydroxy-sodalite membrane, Single gas permeation, Seeding time.*

INTRODUCTION

Zeolites, crystalline aluminosilicates, are widely used in separation and refinery industries as catalysts, adsorbents, membranes and ion exchangers due to their meso and microporous (< 50 nm) structures [1-5]. The significant catalytic activity and selectivity of zeolite materials are attributed to their large internal surface area and highly distributed active sites that are accessible through uniform pore size [6], high thermal resistance; chemical inertness and high mechanical strength [7].

Sodalite is one of the microporous crystalline zeolites which consists of the cubic array of β-cages [8]. Sodalites are microporous tectosilicates with the general composition as Na8[AlSiO4]6(X)2, where X is a monovalent guest anion as chlorine in the mineral

* *To whom correspondence should be addressed.*
+ *E-mail: a.babaluo@sut.ac.ir*
1021-9986/09/4/37 *12/$/3.20*

sodalite [9]. This kind of zeolite has a six-membered ring aperture which these rings of Si_/O_/Si bonds have a pore width of 2.8 Å. Hydroxy-sodalite has the same framework structure as sodalite. The pore size of (hydroxyl-)sodalite is smaller than that of the zeolites with an eight-membered ring aperture, e.g., NaA zeolite, which makes them interesting materials for the separation of small molecules like H_2 or He from various gas or liquid mixtures [10-13]. Therefore, due to the unique applications of hydrogen [14], synthesis of hydroxyl-sodalite membranes for hydrogen purification processes is crucial. Recently, *Xu et al.* [13] synthesized hydroxyl-sodalite/α-Al2O3 composite membrane with a high H_2/n-C_4H_{10} permselectivity.

There are two types of pores in zeolite membranes: 1- intra-crystalline or zeolite pores, 2- inter-crystalline pores [15]. The high potential of zeolite membranes in hydrogen purification process is due to the intra-crystalline pores. Thus, the presence of inter-crystalline pores in the zeolite membrane layers accounts for a considerable decrease in membrane performance. Therefore, elimination of inter-crystalline pores in zeolite membrane layers which causes an increase in their performance in addition to the effects of important factors on the microstructure and performance of the zeolite membranes has a great importance.

In this study, an attempt was made to prepare hydroxy-sodalite zeolite membrane layers on the in-housed manufactured α-alumina tubular supports via hydrothermal secondary growth technique. As mentioned in the literature [16], in this method, various factors such as seed particle size, coating time, coating pressure difference and suspension concentration could significantly affect the final properties of the manufactured membranes. But, due to their importance especially on the membranes microstructure and performance, the first two key factors: seed particle size and coating (seeding) time were considered in our research. Also, the effects of the investigated factors on the single gases (H_2 and N_2) permeation were evaluated under different pressure differences at ambient temperature.

THEORY

In sodalite membrane layers, the hydrogen loading can be expressed as a storage-by-weight percentage by following equation [17]:

$$\text{loading} = \frac{N_{H_2} \cdot M_{H_2}}{\sum_{T=1}^{T=6}(M_T) + N_{H_2} \cdot M_{H_2} + 12M_O + N_{Na} + M_{Na^+}} \times 100\% \quad (1)$$

where N_{H2} is the number of H_2 molecules in the cage [–]; M_{H2} is the molar mass of H_2 [kg/mol]; M_T is the molar mass of the T-atom (T = Si, Al, P, Ge) [kg/mol]; M_O is the molar mass of the O-atom [kg/mol]; N_{Na} is the number of sodium cations [–] and M_{Na} is the molar mass of the sodium cation [kg/mol].

For higher loadings, adsorption isotherms can be represented by the Freundlich isotherm [18]:

$$q = k_F P^{(1/n_F)} \quad (2)$$

For very low loadings, typically <0.2 wt %, adsorption isotherms can be represented by the Henry's isotherm [17]:

$$\frac{q}{qo} = K_H \cdot P \quad (3)$$

where q is the amount of adsorbed H_2 [kg/kg]; qo is the adsorption capacity for H_2 [kg/kg], K_H is the Henry's coefficient and k_F and n_F are empirical parameters.

This set of equations with unknown parameters can be solved by using nonlinear procedures, when a sufficiently large number of empirical data are taken from the adsorption isotherms [17].

On the other hand, two different diffusion regimes were proposed for zeolite (silicalite-1, sodalite, etc.) membranes depending on the temperature: at low temperature, surface diffusion takes place, and at high temperature, gas translation diffusion occurs. Therefore, Bakker et al. model considered only the total permeation flux through the zeolite pores (intra-crystalline pores) as follow [18]:

$$J\big|_{dx} = -\varepsilon\left[\left(\rho q_{sat} D_s^o(\theta=0) e^{-E_{DS}/RT} \frac{1}{1-\theta}\right)\frac{d\theta}{dx} + \left(\frac{\lambda}{z}\sqrt{\frac{8}{\pi MRT}} e^{-E_{DGT}/RT}\right)\frac{dP}{dx}\right] \quad (4)$$

where ε is the porosity of support layer, ρ is the zeolite density, whereas q_{sat} is the saturation capacity and z is a probability factor. Also, four unknown parameters (i.e. $D_s^o(0)$, E_{DS}, λ and E_{DGT}) were presented in Eq. (4) which

can be obtained from independent measurements of the adsorbed amount versus the temperature (isobar at 101 kPa) [18].

The first term in the right hand of Eq. (4) introduces the surface diffusion and the last term is due to the gas translation diffusion which is almost zero at ambient temperature (300K) [18]. Thus, in ambient condition the total permeation flux can be written as:

$$J\Big|_{dx} = -\varepsilon\left[\left(\rho q_{sat} D_s^o(\theta=0) e^{-E_{DS}/RT} \frac{1}{1-\theta}\right)\frac{d\theta}{dx}\right] \qquad (5)$$

Eq. (5) shows that the gas permeation flux through the zeolite membranes is a function of gas adsorption loading (occupancy θ). *Annemieke et al.* calculated hydrogen adsorption isotherms on the sodalite-type structures for the range 73-773 K and 0-3000 bar. Their results showed that the more technologically interesting hydrogen loadings are found only to be achieved under extremely low temperature (< 200 K) and/or extremely high pressure (> 100 bar) conditions. Therefore, the adsorption-diffusion mechanism in sodalite membranes can not be applied in ambient temperature and low pressures. In other words, the single gas permeation flux in ambient conditions is due to the permeability of the inter-crystalline pores. Thus, a further aim of this work was to evaluate the presence of inter-crystalline pores in the manufactured hydroxy-sodalite zeolite membrane layers by the permeation of single gases (H_2 and N_2) under various pressure differences at ambient temperature.

EXPERIMENTAL

Materials

In-housed manufactured gel-casted α-Al_2O_3 porous tubes (12mm outer diameter, 7 mm inner diameter, 2.5 mm in thickness) with an average pore diameter of 570 nm and a porosity of 47 % were used as membrane supports [19].The following chemicals were used for the hydroxy-sodalite zeolite synthesis: sodium hydroxide (NaOH, Merck, > 99 %) aluminum foil (Al, Merck, > 99 %), silica sol ($[SiO_x(OH)_{4-2x}]_n$, Merk, 27 wt. % SiO_2,) and deionized water.

Hydroxy-sodalite seeds synthesis

For the investigation of seeds size and morphology effect, the hydroxyl-sodalite seeds were synthesized via two different routes:

Route 1: The aluminate solution was prepared by dissolving 156 g sodium hydroxide in 300 ml deionized water, then adding 2.1 g aluminum foil to the solution at room temperature. The silicate solution was prepared by mixing 37.5 mL silica sol and 390 mL deionized water at 333K with vigorous stirring. After 10 min of stirring, the preheated aluminate solution was added with mixing for 15 min to produce a clear and homogenous solution. The molar ratio of the final mixture solution was $5SiO_2$:Al_2O_3:$50Na_2O$:$1000H_2O$. The synthesized solution was poured into the Teflon holder of the stainless steel autoclave and heated at 333 K for 24 h.

Route 2: The aluminate solution was prepared by dissolving 10 g sodium hydroxide in 39.75 mL deionized water, then adding 0.25 g aluminum foil to the caustic solution. The silicate solution was prepared by mixing 8.52 g sodium hydroxide, 5.15 mL silica sol and 39.75 mL deionized water. The aluminate solution preheated upto 333 K was added to silicate solution with stirring. In order to produce a clear and homogeneous solution, the resultant mixture was stirred vigorously for 15 min. The molar ratio of the final mixture solution in this route was similar to that of route 1. The solution was poured into Teflon holder of the stainless steel autoclave and heated at 363 K for 6 h.

The hydroxy-sodalite seeds synthesized via both routes were washed several times with deionized water, and then dried in air at 373 K for 3 h.

Support seeding

In-housed manufactured α-Al_2O_3 tubular supports were cleaned with deionized water in ultrasonic cleaner for 5 min to remove the loose particles. Before seeding, the cleaned supports were held in air at 373 K for 3 h. The colloidal suspensions were prepared by dispersing 7 g hydroxy-sodalite seeds in 1000 mL deionized water with ultrasonic treatment.

The seeding layer was coated on the outer surface of the supports by vacuum seeding method using a water pump to create pressure difference between the two sides of support wall. The coating pressure difference was monitored by a pressure gauge. The vacuum seeding was operated under pressure difference of 0.15 bar for different seeding times 60, 120, 180 and 240 s. After vacuum seeding, the seeded supports were dried in air at 373 K for 3 h.

Hydroxy-sodalite top-layer secondary growth

The seeded support was placed vertically with a Teflon holder in a stainless steel autoclave to avoid any precipitation of hydroxy-sodalite zeolite crystals onto the support during the membrane synthesis. The synthesis solutions prepared as mentioned earlier (section: hydroxy-sodalite seeds synthesis), were carefully poured into the autoclave without hitting the support, then the autoclave was sealed. The crystallization was carried out in an air-circulated oven (Route 1: at 333 K for three stages, reaction time 24 h for each stage and Route 2: at 363 K for three stages, reaction time 6 h for each stage). The synthesized hydroxy-sodalite zeolite membrane was washed several times with deionized water, and then dried in air at 373 K for 3 h.

Characterization

The crystalline structure of the synthesized seeds and membranes was determined by X-ray diffraction (XRD) patterns. XRD was carried out on a TW3710 Philips X'Pert diffractometer using CuKα(λ=1.54 Å) radiation operating at 40 kV and 50 mA. Morphology and thickness of the synthesized hydroxy-sodalite zeolite membranes were examined by scanning electron microscope (SEM, LEO 440I, 3×10^5, LEO, UK).

Single gas permeation

Single gas permeation measurement was carried out in ambient conditions to evaluate the quality and inter-crystalline structure of the hydroxy-sodalite zeolite membranes. The synthesized hydroxy-sodalite zeolite membranes were sealed in a permeation module with the zeolite membrane facing the high-pressure side. Measurements of H_2 and N_2 permeation were made at ambient temperature (283 K) and at pressure differences up to 6 bar. Permeance was measured using the stainless steel permeator shown schematically in Fig. 1. Both annular ends between the membrane tube and the permeator wall were sealed with moulded RTV silicone gasket rings. Feed gas flowed along the outside of the membrane and the permeated gases were measured on the inner side of the membrane at pressure 1 bar. Pressure differences across the membrane were obtained by varying the pressure on the upstream side and keeping the pressure constant on the downstream at 1 bar. Pressure in the shell side of the membrane module was monitored via a pressure gauge.

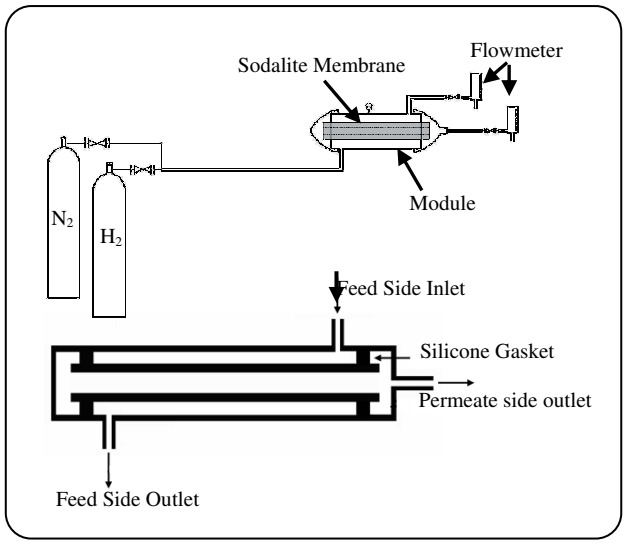

Fig. 1: Schematic of a tubular permeator.

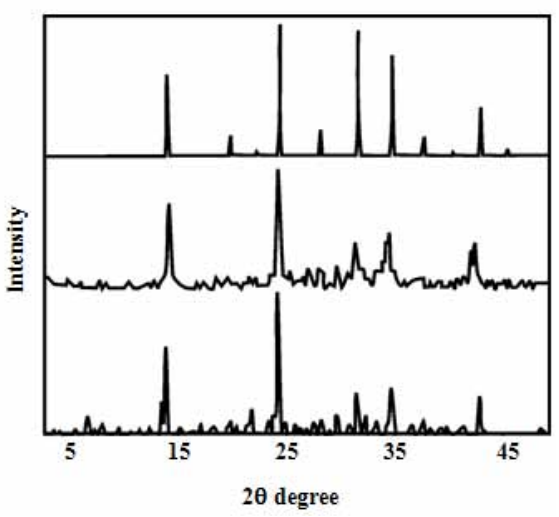

Fig. 2: XRD patterns of the synthesized hydroxy-sodalite zeolite seeds; a) route 1, b) route 2 and c) standard hydroxy-sodalite.

RESULTS AND DISCUSSION

Synthesized hydroxy-sodalite seeds

The synthesized hydroxy-sodalite seeds were characterized by XRD and SEM. The XRD patterns of the synthesized hydroxy-sodalite zeolite with both routes have been compared with standard hydroxy-sodalite XRD pattern which confirms the synthesis of hydroxy-sodalite zeolite (see Fig. 2). SEM micrographs and morphology of the hydroxy-sodalite zeolite seeds synthesized with both routes have been presented in Fig. 3. As illustrated in this figure, the morphology of hydroxy-sodalite zeolite synthesized via first route is

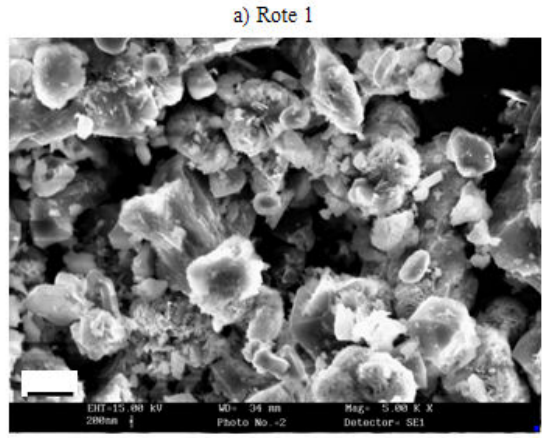

Fig. 3: SEM micrograph of the synthesized hydroxy-sodalite zeolite seeds.

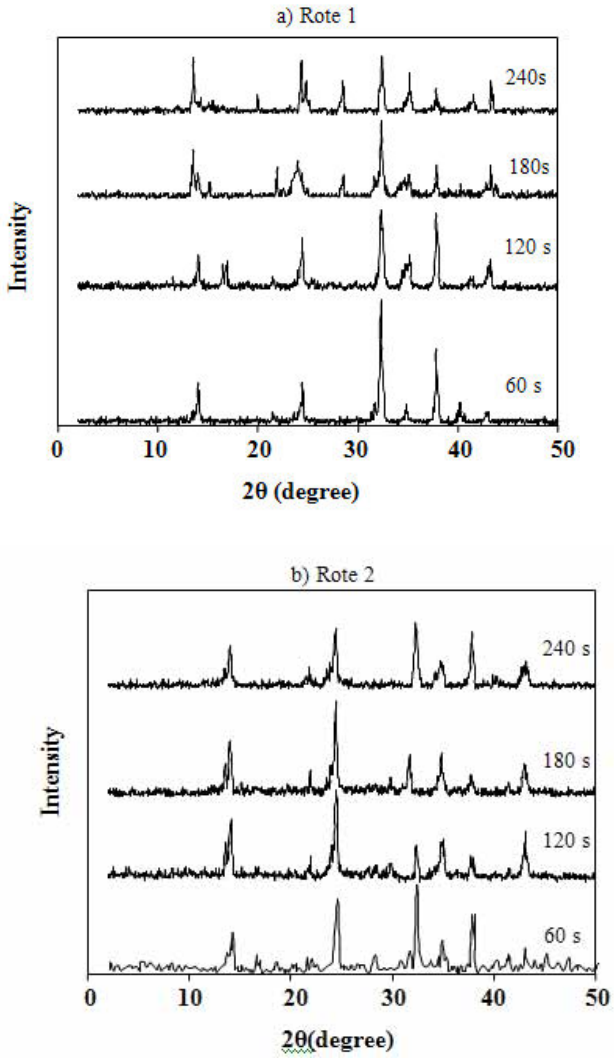

Fig. 4: XRD patterns of the synthesized membranes with different seeding times.

completely irregular and has a particle size of 1-1.5 µm, whereas hydroxy-sodalite seeds synthesized via the second route have an absolutely spherical structure with a monodispersed particle size of 10 µm. Synthesis of hydroxy-sodalite seeds with different particle size and morphology can be due to the difference in the not only preparation of synthesis solutions but also crystallization time and temperature.

Synthesized hydroxy-sodalite membranes

The XRD patterns of the manufactured sodalite membranes with different seeding times for both routes have been presented in Fig. 4. It is found that the thin films formed on the α-Al_2O_3 supports surface are hydroxy-sodalite zeolite.

Figs. 5 and 6 show the SEM micrographs of top-views and cross-sections of the prepared membranes via the first route. As can be seen, membrane manufactured with seeding time of 60 s has a more compact and uniform layer. However, according to the literature [20], XRD and SEM characterization methods can only indicate whether a continuous membrane is formed on the support or not, but they cannot confirm whether a defect-free zeolite membrane is formed or not. Such a property of defect-free zeolite membrane can only be evaluated by the gas permeation test.

The top-view and cross-section SEM images of the synthesized membranes on the seeded α-Al_2O_3 support with different seeding times via the second route have been presented in Figs. 7 and 8.

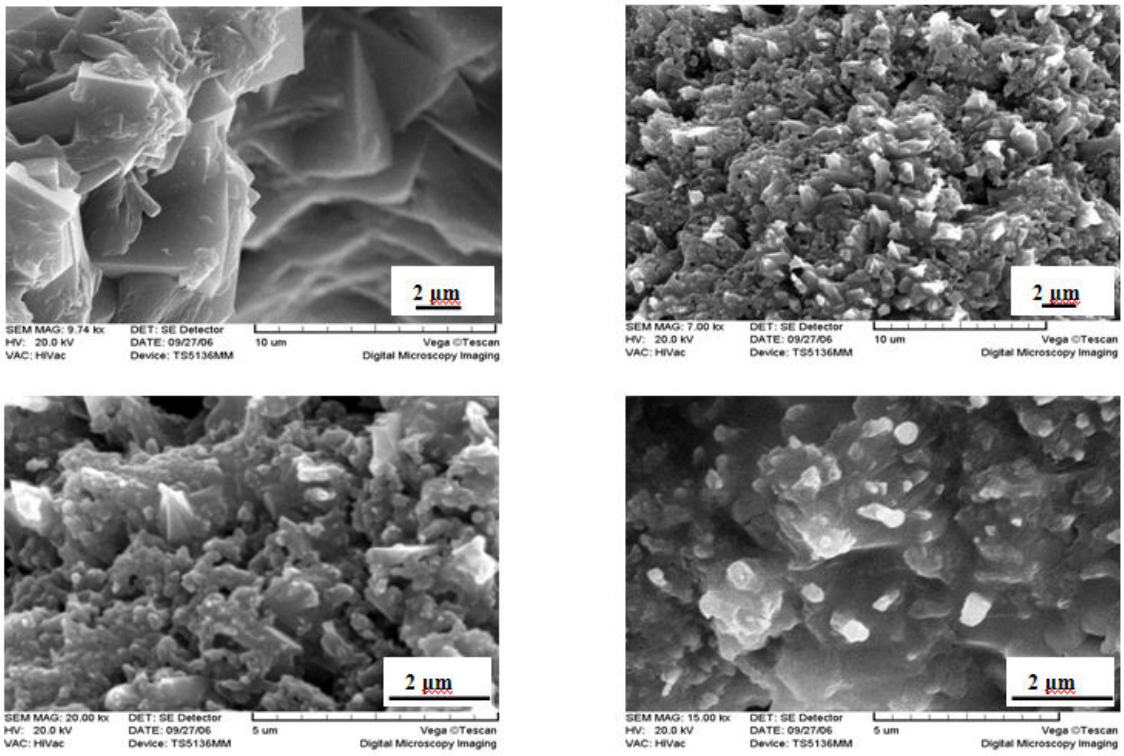

Fig. 5: Top-view SEM micrographs of the membranes top-layers prepared with the first route at seeding time: a) 60 s, b) 120 s, c) 180 s and d) 240 s.

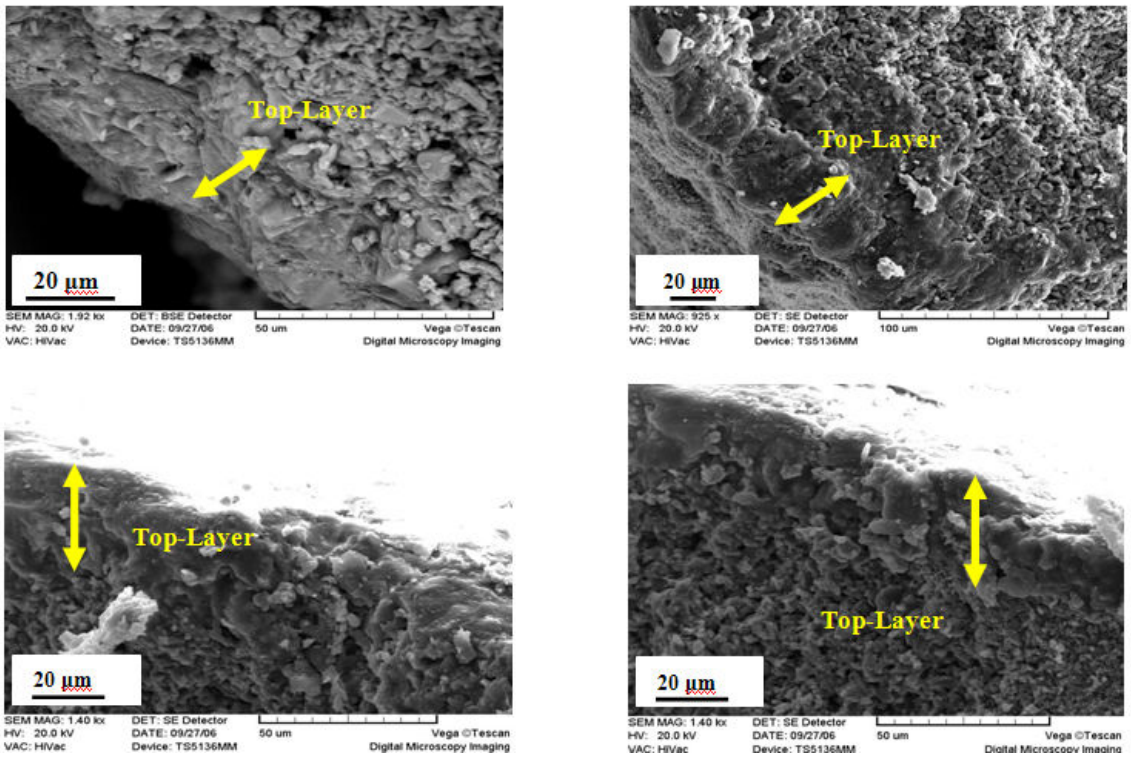

Fig. 6: Cross-section SEM micrographs of the membranes top-layers prepared with the first route at seeding time: a) 60 s, b) 120 s, c) 180 s and d) 240 s.

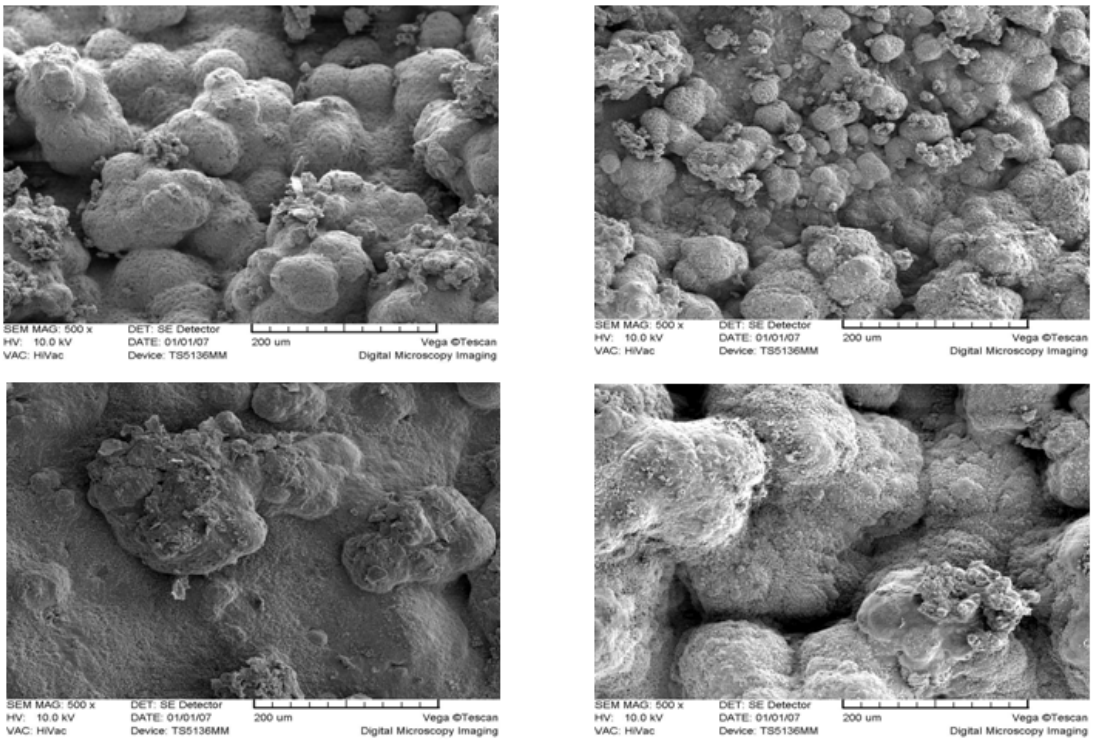

Fig. 7: Top-view SEM micrographs of the membranes top-layers prepared with the second route at seeding time: a) 60 s, b) 120 s, c) 180 s and d) 240 s.

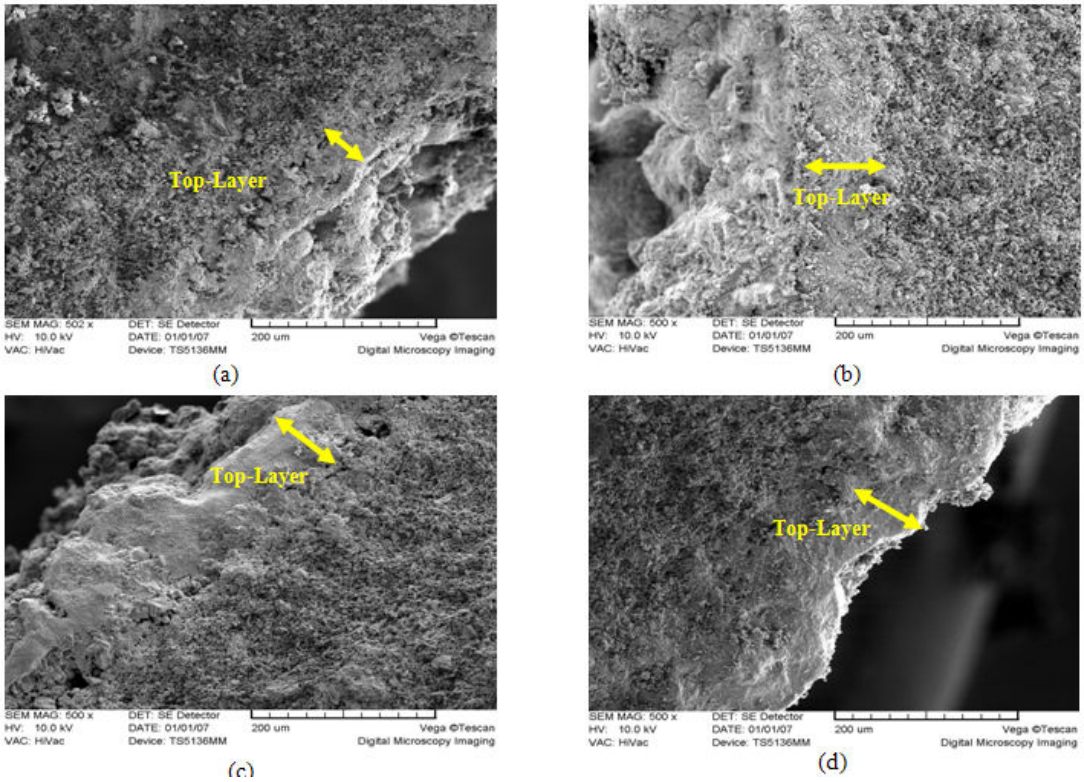

Fig. 8: Cross-section SEM micrographs of the membranes top-layers prepared with the second route at seeding time: a) 60 s, b) 120 s, c) 180 s and d) 240 s.

As can be seen, all the supports are covered with a uniform layer of hydroxy-sodalite zeolite, but since the crystal size in this route is much larger than that of the first route, the comparison between the uniformity of layers is not possible. Thus, Fig. 9 has been given to observe the microstructures of the hydroxy-sodalite layers cross-sections. It can be found that low-compact top-layer was formed in the membranes manufactured with seeding time 180s.

The obtained results showed that by increasing seeding time, thickness of hydroxy-sodalite layers increases dramatically and a maximum thickness was obtained at seeding time 120 s and 180 s for routes 1 and 2, respectively. As shown in Fig. 9, further increase in seeding time causes to form compact top-layers with the same thickness.

The effect of seeding time on zeolite membranes thickness is not well established. But, as mentioned in literature, at low seeding time the support surface was not completely covered by a continuous seeding layer [16]. However, at seeding time in the range of 60-90 s, a uniform seeding layer and finally a compact and continuous zeolite membrane layer was formed on support surface. By increasing of seeding time, the support surface was covered by zeolite seeds with multilayer structure, and zeolite membrane layers were constructed with high thickness and porosity. By further increasing of seeding time, although the applied vacuum was not be able to increase thickness of the seeded layers, but relatively compact layers of zeolite seeds with a fixed thickness were formed on support surface during the long seeding time. Similar structure was observed in the final zeolite membrane layers.

However, permeation test was carried out in order to attain a more exact comparison of either the two routes or seeding times.

Single gas permeation studies

Besides qualitative characterization, the permeability of the manufactured hydroxy-sodalite membranes was measured. The permeation of single gases (H_2 and N_2) as a function of pressure difference at ambient temperature for the manufactured membranes with different seeding times has been depicted in Figs. 10 and 11 for routes 1 and 2, respectively.

It is notable that since the adsorption of gases (hydrogen) on hydroxy-sodalite zeolite is very low inambient conditions [17, 18], the flux of gases passing through the membrane is due to inter-crystalline pores. Hence, membranes having lower permeability in these conditions are more desirable because of their lower inter-crystalline pores.

The relation for the permeance of gases through inter-crystalline pores of the manufactured hydroxy-sodalite membranes can be obtained as follow:

$$\text{Permeance}\left(\frac{\text{mol}}{\text{m}^2\cdot\text{s}\cdot\text{Pa}}\right)=\frac{1}{R_k}+\frac{\overline{P}}{R_p} \qquad (6)$$

where R_k is the Knudsen resistance and R_p is the Poiseuille resistance defined independent of the pressure conditions [21, 22]. Therefore, the values of the gas permeance are linear function of the arithmetic mean gas pressure in permeator ($\overline{P}$) as shown in Figs. 12 and 13. Also, the permselectivity of H_2/N_2 binary gas mixture was presented in Fig. 14 as a function of pressure difference, which shows an ideal selectivity about 2.1-2.5. As mentioned in literature [17, 18], the effect of adsorption/diffusion mechanism on the permeation flux of single gases through the hydroxy-sodalite zeolite membranes can be negligible at ambient conditions. In the other words, the single gas permeation flux through our manufactured membranes at ambient conditions can be attributed to transition flow mechanism (both viscous flow and Knudsen diffusion).

As shown in Figs. 12-14, in the first route, a maximum permeation is observed in the seeding time of 120 s, whereas in the second route, the maximum point can be seen in 180 s. But, the seeding time does not have significant effect on the selectivity (see Fig. 14). According to SEM micrographs, these findings can be due to the top-layers microstructure formed at different seeding times, so that top-layers with the lower compact contain the higher inter-crystalline pores and thus the higher permeation.

Comparing the permeation of the membranes manufactured with two different routes, it can be inferred that the flux of gases passing through the membrane prepared by the first route is lower and thus, under extremely low temperatures (< 200 K) and/or extremely high pressures (> 100 bars), better results can be achieved for hydrogen purification via this route.

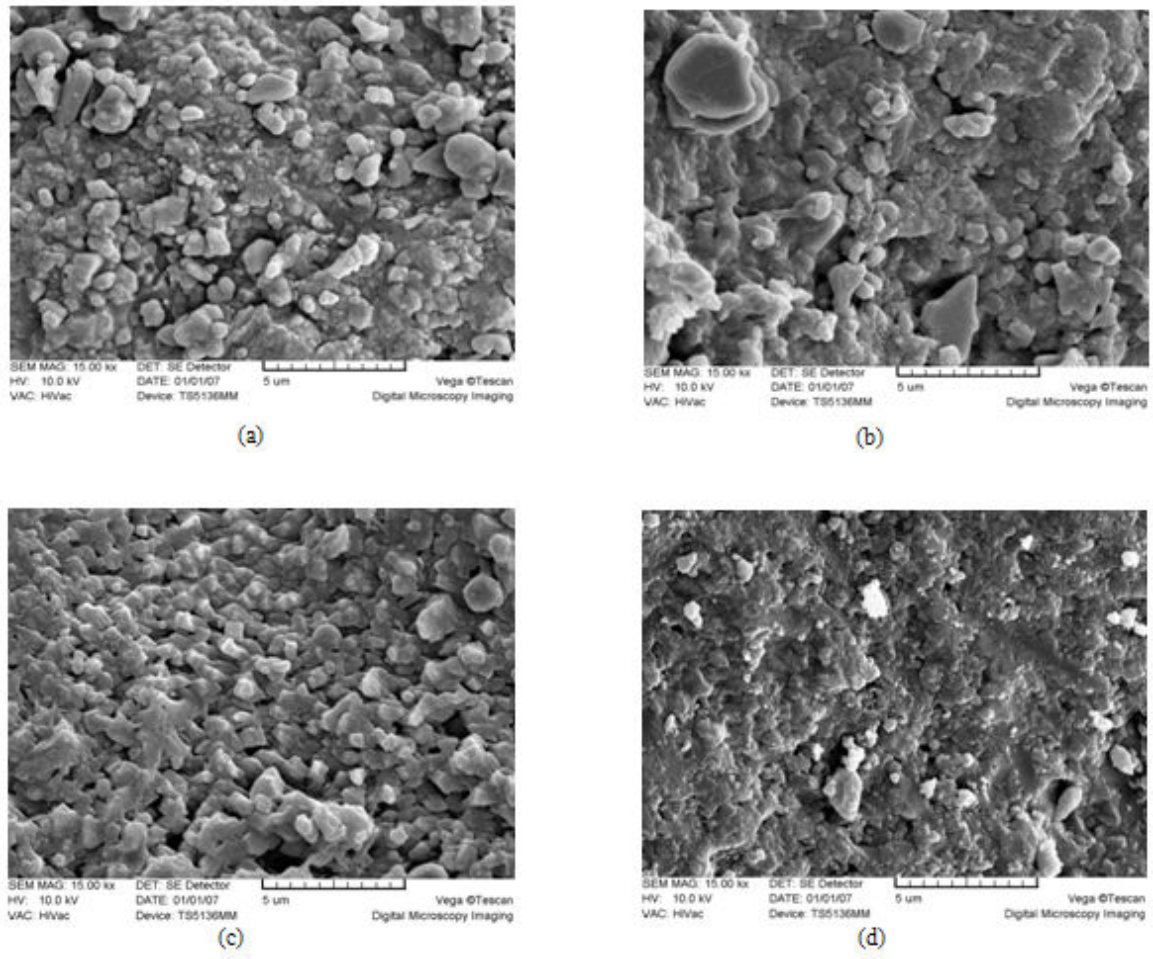

Fig. 9: Cross-section microstructure of the membranes top-layers prepared with the second route at seeding time: a) 60 s, b) 120 s, c) 180 s and d) 240 s.

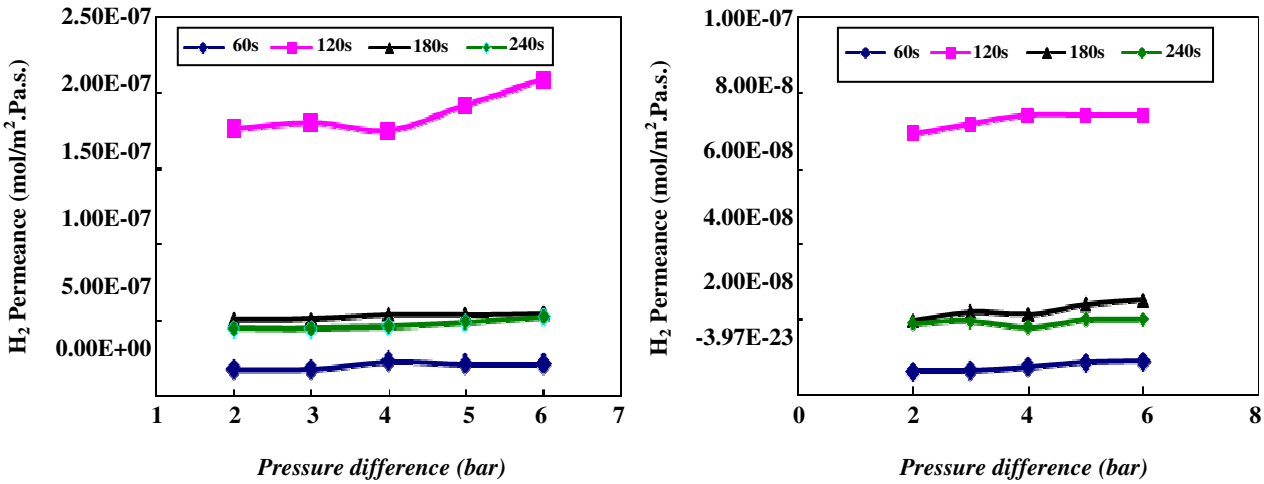

Fig. 10: Permeance of the synthesized membranes with route1 for a) H_2 and b) N_2 as a function of pressure difference at different seeding times.

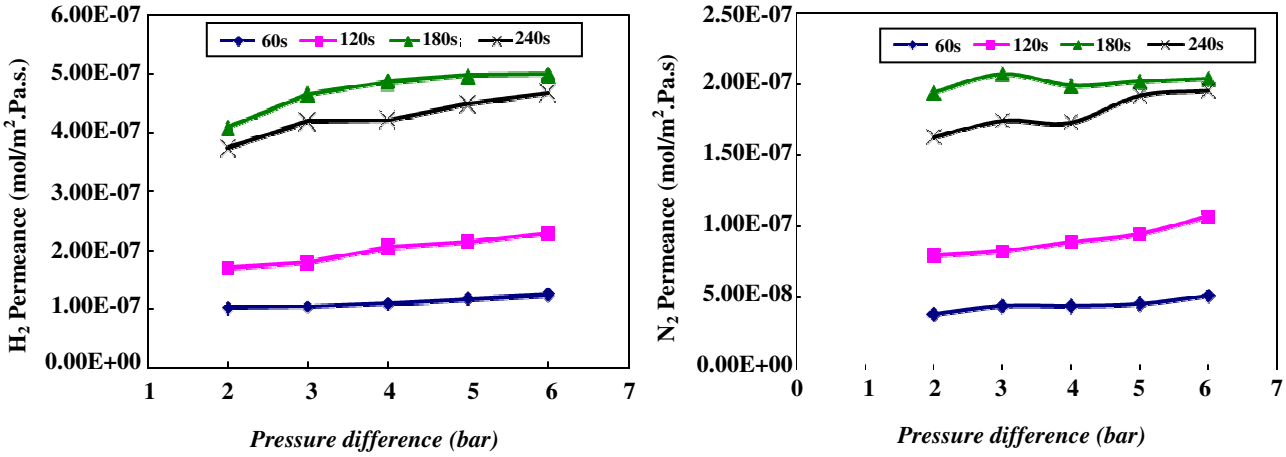

Fig. 11: Permeance of the synthesized membranes with route 2 for a) H_2 and b) N_2 as a function of pressure difference at different seeding times.

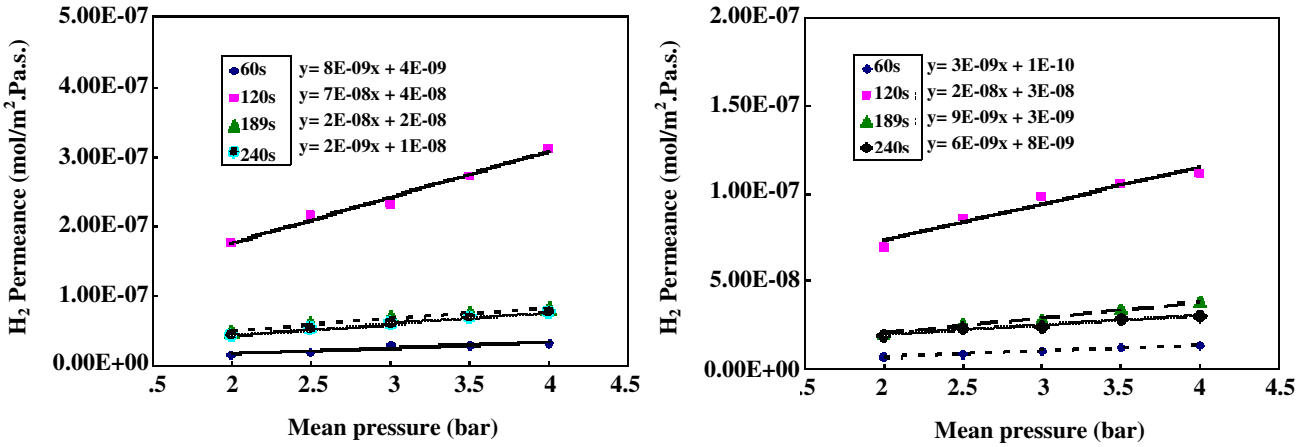

Fig. 12: Permeance of the synthesized membranes with route1 for a) H_2 and b) N_2 as a function of mean pressure at different seeding times.

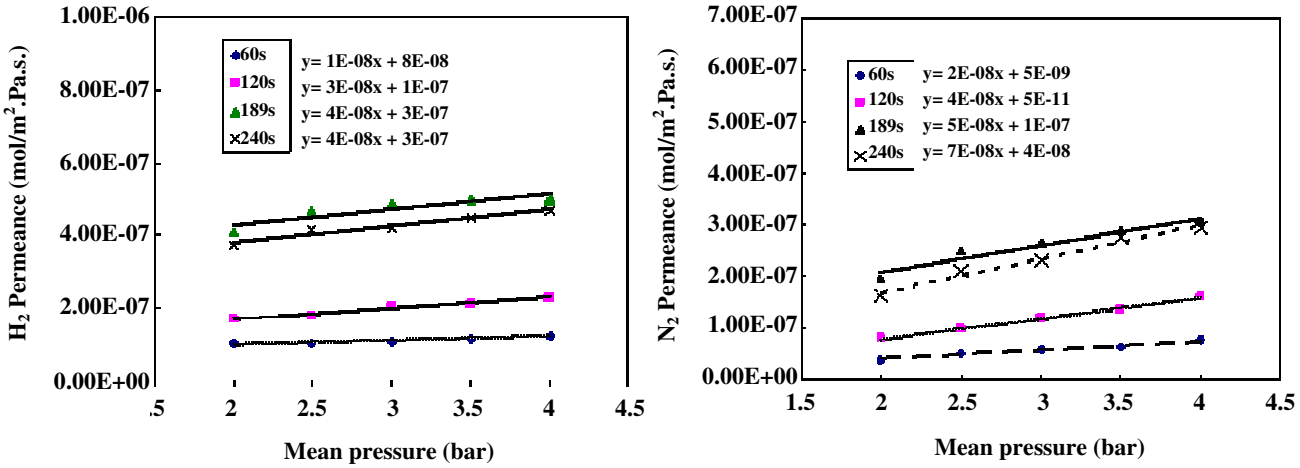

Fig. 13: Permeance of the synthesized membranes with route2 for a) H_2 and b) N_2 as a function of mean pressure at different seeding times.

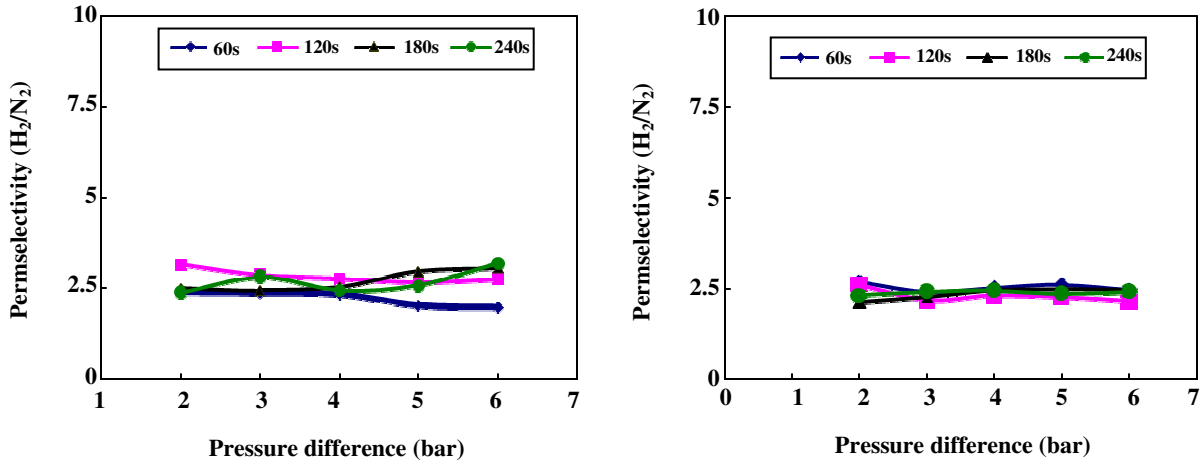

Fig. 14: Permselectivity of the membranes synthesized with a) route 1 and b) route 2 for H_2/N_2 binary mixture as a function of pressure difference at different seeding times.

More details on the performance of these membranes for hydrogen purification at low temperatures (< 200 K) are under investigation.

CONCLUSIONS

The obtained results in this work are presented as follows:

- Microporous sodalite membranes with uniform structures were successfully synthesized on α-Al_2O_3 tubular supports from synthesis mixtures with the aid of nucleation seeds via two different routes.

- A more compact and uniform sodalite membrane layers were synthesized via the first route at seeding time of 60 s and a relatively similar trend was observed with more detailed studies in the second route.

-Single gas permeation of the manufactured sodalite membranes were studied in ambient conditions. The obtained results showed that in the gas permeation through inter-crystalline pores of the manufactured sodalite membranes both viscose flow and Knudsen diffusion mechanisms have influence (i.e. transition flow mechanism).

- Due to the permeation of single gases through inter-crystalline pores of sodalite membranes in ambient conditions, it can be concluded that the membranes prepared via the first route at seeding time 60 s, is proposed for hydrogen purification processes under extremely low temperatures (< 200 K) and/or extremely high pressures (> 100 bars).

Acknowledgments

The Authors wish to thank Sahand University of Technology (SUT) and Tabriz refinery for the financial support of this work. Also, thank co-workers and technical staff in the chemical engineering department, polymer engineering department, Institute of polymeric materials and nanostructure materials research center of SUT for their help during various stages of this work.

Nomenclatures

J	Molar flux through membrane (mol m^{-2} s^{-1})
K_H	Henry's coefficient
k_F	Empirical parameters
M_{Na}	Molar mass of the sodium cations (kg/mol)
M_{H2}	Molar mass of H_2 (kg/mol)
M_T	Molar mass of the T-atom (T = Si, Al, P, Ge) (kg/mol)
M_O	Molar mass of the O-atom (kg/mol)
N_{H2}	Number of H_2 molecules in the cage (–)
N_{Na}	Number of sodium cations (–)
n_F	Empirical parameters
q	Amount of adsorbed H_2 (kg/kg)
q0	Adsorption capacity for H_2 (kg/kg)
q_{sat}	Saturation capacity (kg/kg)
z	Probability factor
ε	Porosity of support layer
ρ	The zeolite density (kg/cm^3)

Received : 29th May 2008 ; Accepted : 27th January 2009

REFERENCES

[1] Modirshahla, N. and M. Tabatabaii, S., Removal of Emulsified and Dissolved Traces of Organic Compounds from Industrial Wastewaters Using Natural and Synthesized (NaA and NaM) Zeolites, *Iran. J. Chem. & Chem. Eng.* (*IJCCE)*, **23** (2004).

[2] Sathupunya, M., Gulari, E. and Wonghasemjit, S., ANA and GIS Zeolite Synthesis Directly from Alumatrane and Silatrane by Sol-Gel Process and Microwave Techniques, *J. Eur. Ceram. Soc.,* **22**, 2305 (2002).

[3] Sathupunya, M., Gulari, E. and Wonghasemjit, S., Na-A (LTA) Zeolite Aynthesis Directly from Alumatrane and Silatrane by Sol-Gel Microwave Techniques, *J. Eur. Ceram. Soc.,* **23**, 1293 (2003).

[4] Tavolaro, A. and Drioli, E., Zeolite Membrane, *Adv. Mater.,* **11**, 975 (1999).

[5] Kazemimoghadam, M. and Mohammadi, T., Synthesis of MFI Zeolite Membranes for Water Desalination, *Desalination,* **206**, 547 (2007).

[6] Chen, L. and Deem, M.W., Strategies for High Throughput, Templated Zeolite Synthesis, *Molec. Phys*., **100**, 2175 (2002).

[7] Xu, X., Yang, W., Liu, J. and Lin, L., Synthesis of NaA Zeolite Membranes from Clear Solution, *Micropor. Mesopor. Mater*., **43**, 299 (2001).

[8] Buhl, J. C. and Lons, J., Synthesis and Crystal Structure of Nitrate Enclathrated Sodalite Na 8 [A1SiO4]6 (NO3) 2, *J. Alloy. Comp*., **41**, 235 (1996).

[9] Buhl, J.C., Gesing, T.M., Kerkamm, I. and Gurris, C., Synthesis and Crystal Structure of Cyanate Sodalite Na 8 (OCN)2j[Al6Si6O24], *Micropor. Mesopor. Mater*., **65**, 145 (2003).

[10] Julbe, A., Motuzas, J., Cazevielle, F., Volle, G. and Guizard**,** C., Synthesis of Sodalite/α-Al_2O_3 Composite Membranes by Microwave Heating, *Sep. Purif. Technol.,* **32**, 139 (2003).

[11] Van Niekerk, A., Zaha, J., Breytenbach, J. C. and Krieg, H. M., Direct Crystallization of a Hydroxyl Sodalite Membrane without Seeding using a Conventional Oven, *J. Membr. Sci*., **300**, 156 (2007).

[12] Khajavi, S., Kapteijn, F. and Jansen, J. C., Synthesis of thin Defect-Free Hydroxy Sodalite Membranes: New Candidate for Activated Water Permeation, *J. Membr. Sci.,* **299**, 63 (2007).

[13] Xu, X., Bao, Y., Song, C., Yang, W., Liu, J. and Lin, L., Microwave-assisted Hydrothermal Synthesis of Hydroxy-Sodalite Zeolite Membrane, *Micropor. Mesopor. Mater.,* **75**, 173 (2004).

[14] Manna, G.L., Barone, G., Varga, Z.and Duca, D., Theoretical Evaluation of Structures and Energetics Involve in the Hydrogenation of Hydrocarbons on Palladium Surfaces, *J. Molec. Struc*., **548**, 173 (2001).

[15] Titus, M. P., Llorens, J., Tejero, J. and Cunill, F., Description of the Pervaporation Dehydration Performance of A-Type Zeolite Membranes: A Modeling Approach Based on the Maxwell-Stefan Theory, *Catal. Today*, **118**, 73 (2006).

[16] Huang, A., Lin, Y.S. and Yang, W., Synthesis and Properties of A-Type Zeolite Membranes by Secondary Growth Method with Vacuum Seeding, *J. Membr. Sci*., **245**, 41 (2004).

[17] Van den Berg, A.W.C., Bromley, S. T., Wojdel, J. C. and Jansen, J. C., Adsorption Isotherms of H_2 in Microporous Materials with the SOD Structure: A Grand Canonical Monte Carlo Study, *Micropor. Mesopor. Mater*., **87**, 235 (2006).

[18] Luca, G.D., Pullumbi, P., Barbieri, G., Famà, A.D., Bernardo, P. and Drioli, E., Gusev and Suter Calculation of the Diffusion Coefficients of Light Gases in Silicalite-1 Membrane and Silica-Sodalite Zeolite, *Sep. Purif. Technol*., **36**, 215 (2004).

[19] Bayati, B. and Babaluo, A.A., Manufacturing Porous Supports of Ceramic Membranes and Debinding Behavior in Gel-Casting Method, 11th Chemical Engineering Congress, Tarbiat Modares University, Tehran, Iran, November (2006).

[20] Xu, X., Yang, W.and Liu, J., Synthesis and Gas Permeation Properties of an NaA Zeolite Membrane, *Chem. Commun*., **603** (2000).

[21] Uchytil, P. and Broz, Z., Gas Separation in Ceramic Membranes Part I. Theory and Testing of Ceramic Membranes, *J. Membr. Sci*., **97**, 139 (1994).

[22] Uchytil, P. and Broz, Z., Gas Separation in Ceramic Membranes Part II. Modeling of Gas Permeation Through Ceramic Membrane with one Supported Layer, *J. Membr. Sci.*, **97**, 145 (1994).